Optik 140 (2017) 584–591

Contents lists available at ScienceDirect

Optik

journal homepage: www.elsevier.de/ijleo

Original research article

Power scaling of end-pumped Nd:YLF lasers, modeling and experiments

R.M. El-Agmy[a,*], N. Al-Hosiny[b,c]

[a] Helwan-University, Faculty of Science (Physics) 11792 Helwan, Egypt
[b] Department of Physics, Faculty of Science, Aljouf University, Sakkaka, Saudi Arabia
[c] Department of Physics, Faculty of Science, Taif University, Taif, Saudi Arabia

ARTICLE INFO

Article history:
Received 28 January 2017
Accepted 23 April 2017

Keywords:
Solid state lasers
Thermally induced lens
Wavefront sensors

ABSTRACT

Numerical modeling simulations are carried out to analyze and study the thermal effects in Nd:YLF laser crystals. The distributions of temperature and stress in the Nd:YLF laser rods are calculated with finite element (FE) simulations for different rod geometries and pump powers. The FE simulations that were carried out showed that using thinner Nd:YLF rod would lead to scale the power by 50% before the limits imposed by the thermally induced stress is reached. Also, we have investigated the generation of strong negative thermally induced lens for π- polarizations. The calculations of thermally induced lens in Nd:YLF laser rod is validated experimentally. Shack-Hartmann wavefront sensor was used for direct measurements of thermal lenses at different pump power. The obtained measurements were coinciding with the (FE) simulations.

1. Introduction

Neodymium (Nd) doped yttrium lithium fluoride (YLF) has been used as a continuous wave (CW) and Q-switched laser source for numerous applications in scientific, industrial and medical fields due to its desired thermo-optical properties [1–5]. This properties represented in weak thermal lensing provides for a high quality, free depolarization effect that hindered the output power due to its birefringence nature [1,6]. However, Tm:YLF suffers a low thermally-induced stress fracture limit [7], restricting to its power-scalability. Some approaches to solve this problem in end pumped Nd:YLF lasers, is to increase the length of the gain medium and to lower the doping or to decrease the width of the gain medium and to increase the doping (thin disk lasers [8]). However, no balance between efficiency and thermal effect can be found if the thermal effects are incomplete and are not incorporated in a laser design [9–13]. Rare experimental and theoretical discussions in other papers so far we know for the dependence on the pump beam size, rod diameter and pump distributions that can be utilized for optimization for power scaling which is the aim of this work. In the present work, we have investigated power limits imposed by thermally induced stress in Nd:YLF rods which eventually can lead to the fracture of the rod under different pump powers and rod geometries using finite element (FE) simulation LASCAD program [14]. Also, we have presented the FE simulations for temperature distributions as well as thermal focal length of thermally induced lens. The numerical simulations showed that reducing Nd:YLF rod diameter by 25% would lead to scale the power limit before fracture occurs by 50%. The FE calculations were validated experimentally using Shack-Hartmann wavefront sensor. We have introduced direct

* Corresponding author.
E-mail addresses: Redaagmy@science.helwan.edu.eg, Redaagmy@yahoo.com (R.M. El-Agmy).

http://dx.doi.org/10.1016/j.ijleo.2017.04.087
0030-4026/

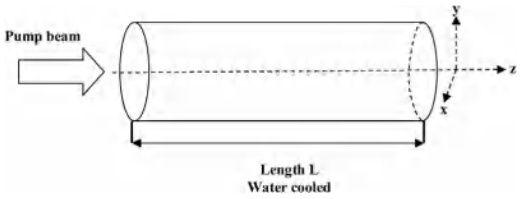

Fig. 1. The model for end-pumped Nd:YLF laser rod.

Table 1
The Nd:YLF parameters used in the finite-element analysis [12,16].

Refractive index	σ	1.448
	π	1.47
Thermo-optical coefficient dn/dt (10^{-6}/k)	σ	-2
	π	-4.3
Heat conductivity (W/mK)	6.3	
Thermal expansion coefficient (10^{-6}/K) z-axis	8.3	
Young's modulus (GPa)	85	
Poisson's ratio	0.33	
Percent of absorbed pump power	85%	
Fraction of absorbed power which is converted to heat under lasing condition	32%	

and accurate measurements for thermal focal length of thermally induced lens at different pump power for π-polarizations. The obtained measurements were coinciding with the (FE) simulations.

2. FE model considerations

The model assumes that a Nd:YLF rod as sketched in Fig. 1. The barrel of the copper is water-cooled ($T_{coolant} = 291\,K$) and the front and back faces are in contact with air, the heat transfer coefficients for water and air cooling were set to be $h = 2.0\,W\,cm^{-2}\,K^{-1}$ and $h = 0.005\,W\,cm^{-2}\,K^{-1}$, respectively [14].

The temperature dependence of the heat conductivity was taken into account. Low dopant concentration 0.7% (at.) Nd^{+3} was used in the (FE) calculations to reduce the fracture risk of Nd:YLF laser rod and possible up-conversion processes instead of the typical ~1–1.2% [2]. Pump wavelength of 805 nm was chosen which has a low absorption cross section as compared to peak absorption at 793–797 nm to avoid thermal fracture with intensive diode pumping [9]. An additional concern in reducing pump intensity while maintaining diffraction limited fundamental mode oscillation TEM_{00} is that the Nd:YLF radius is much larger (~3 times [2,10]) than pump radius. The simulated length Nd:YLF laser rod is chosen according to attenuation law:

$$I(z) = I_0 e^{-z\alpha} \tag{1}$$

Where *I(z)* is the intensity of the pump light inside Nd:YLF laser rod along its z-axis, α is the absorption coefficient and I_0 is the initial pump intensity. With the above equation and ($\alpha \sim 1.1\,m^{-1}$ [15]), one gets the length Nd:YLF laser rod of 10 mm. Four Nd:YLF rods with diameters 1, 2, 3, 4 mm were analyzed for pump powers ranged 5–55 W. The Nd:YLF parameters used in the FE simulations are given in Table 1. Also we assumed a uniform pump configuration with pump radius of 300-μm to avoid asymmetric thermally induced lens.

3. FE simulation results and discussion

3.1. Temperature distributions in end-pumped Nd:YLF laser rods

Fig. 2(a–d) shows FE simulations of the temperature distribution on the y-z plane in end pumped Nd:YLF lasers rods at 25 W for rod length 10 mm and diameters 4, 3, 2 and 1 mm, respectively. Only the upper half of the rod is shown due to symmetry.

The pump beam is focused at the rod end, the results allow a detailed analysis of the temperature distribution within the crystals, and different colors indicate the different temperatures. The highest temperature is found where the pump beam enters the Nd:YLF rod, which also indicates where most of the pump photons are absorbed. It also decreased in the propagation direction as the pump was absorbed.

Fig. 3 shows the central temperature of Nd:YLF rods of length 10 mm verses pump powers and different diameter. The slope was found to be 2.8 K/W, 2.6 K/W 2.2 K/W and 1.3 K/W of Nd:YLF rod with diameter of 4 mm, 3 mm, 2 mm and 1 mm, respectively. It is clearly seen that, by simply reducing rod diameter from 4 mm to 1 mm the thermal load decreased by almost a factor of ½. This is mainly due to rod conducive to cooling.

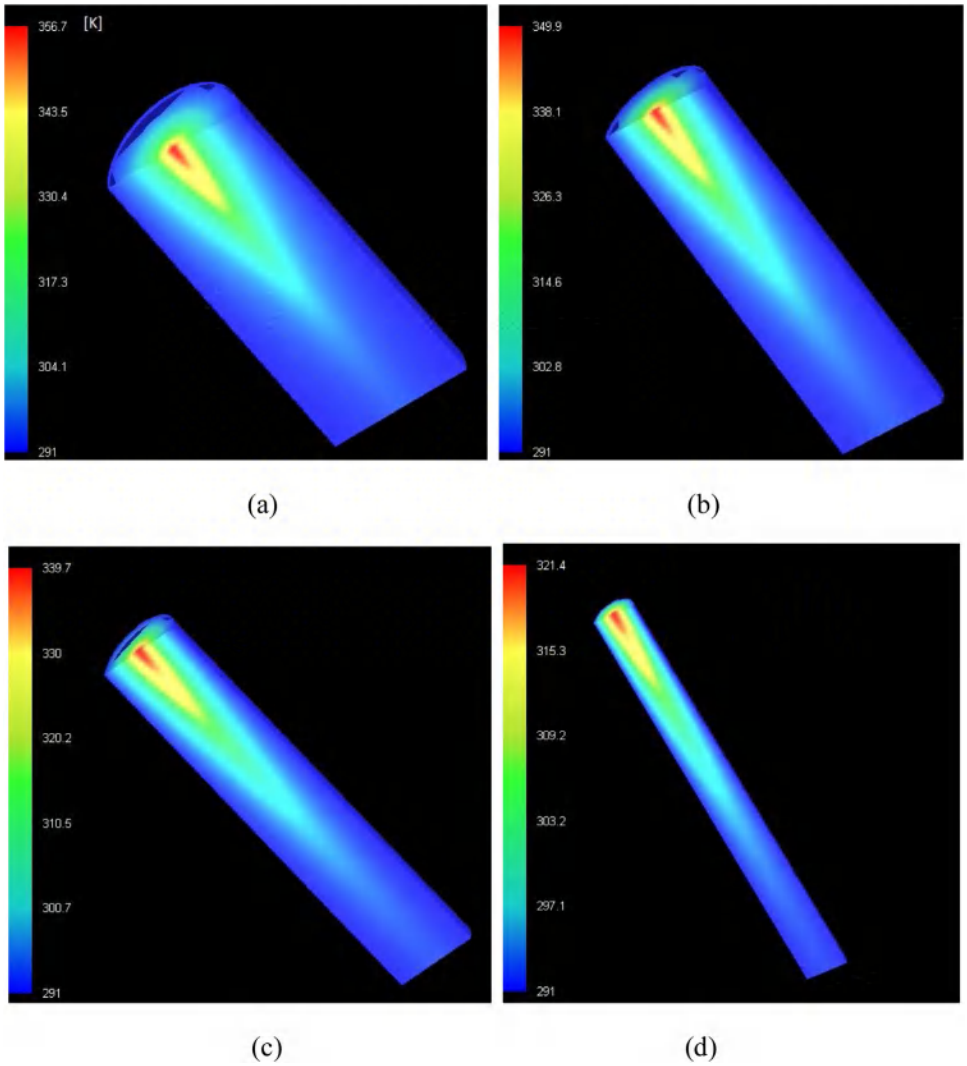

Fig. 2. Numerically calculated temperature distribution for end pumped Nd:YLF rods of length 10 mm and diameters (a) 4 mm, (b) 3 mm, (c) 2 mm and (d) 1 mm, at 25W of pump power.

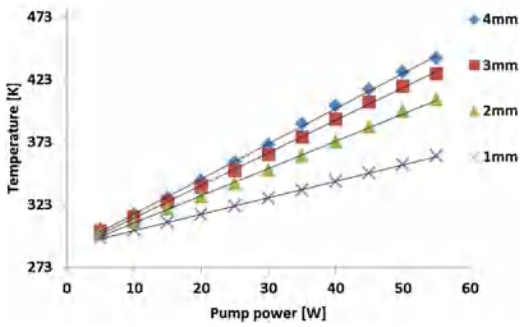

Fig. 3. Variations of the central temperature versus pump power ranged from 5 to 55 W for Nd:YLF rods of length 10 mm and different rod diameters 4 mm, 3 mm, 2 mm, and 1 mm.

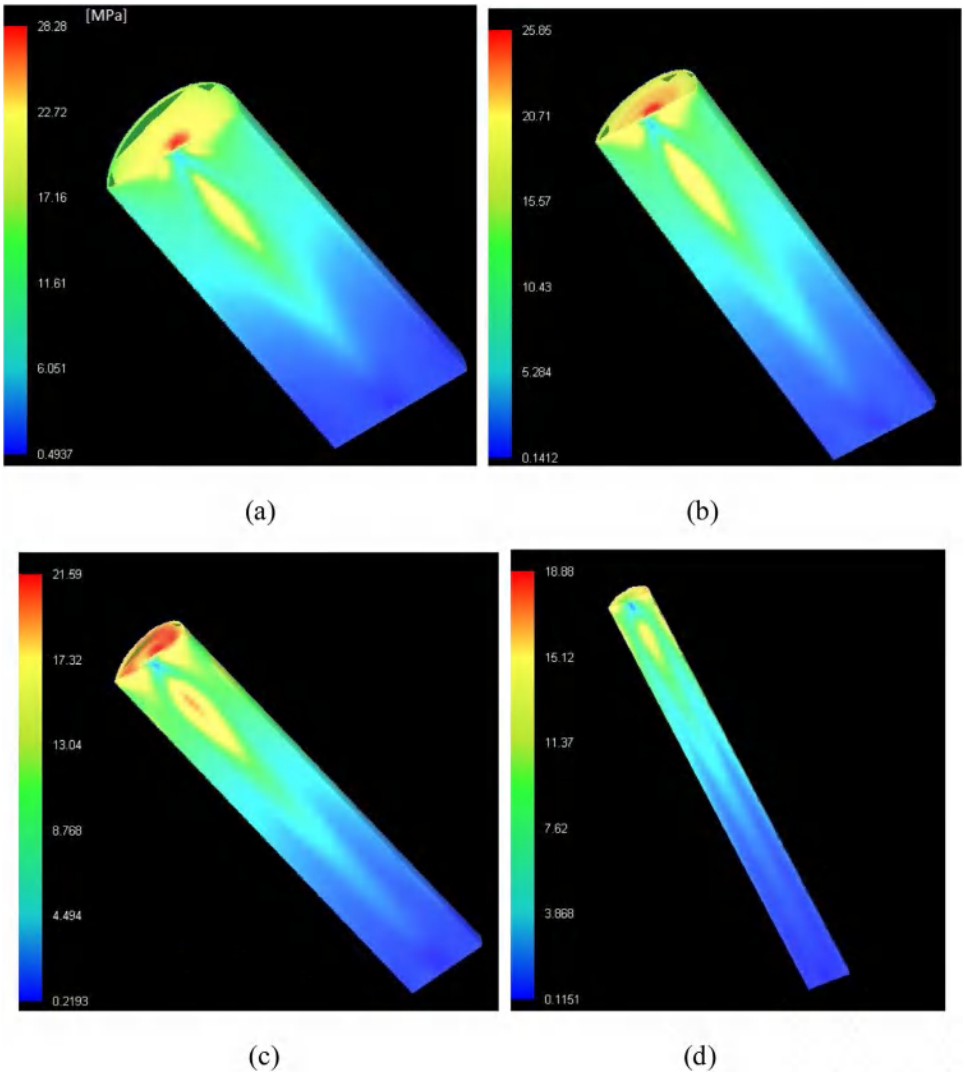

Fig. 4. Numerically calculated stress intensity distribution for end pumped Nd:YLF rods of length 10 mm and diameters (a) 4 mm, (b) 3 mm, (c) 2 mm and (d) 1 mm, at 25W of pump power.

3.2. Thermally induced stress and power scaling

Since the fragile nature of YLF crystals, it's essential to predict the maximum pump powers before fracture occurs. In the following, we present calculation of (FE) simulations to evaluate the power limits imposed by thermally induced stress which eventually can lead to the fracture of the rod. The nonuniform temperature distribution results in mechanical stress and strain. Fig. 4(a–d) shows the FE simulation results of stress intensity for Nd:YLF rod of different diameters (a) 4 mm, (b) 3 mm, (c) 2 mm and (d) 1 mm, pumped at 25 W. The real amount and the spatial distribution of the stress intensity depend on the temperature distribution as well as on the material constants. The highest stress intensity is clearly on the center top and bottom positions of the crystal. We could therefore expect thermally induced crack formation to start from these positions where the stress is showing to be high.

Fig. 5(a–d) shows plots of the maximum stress intensity in the Nd:YLF at different pump powers and rod diameters. As can be seen in Fig. 5 that linear increase in the maximum stress intensity as a function of pumps powers. The stress intensity rise is a function of the temperature difference between the rod center and its circumference while the all other parameters of rod length, material parameters, a fractional heat load of 32% due to the quantum defect heating are fixed for comparison. As mentioned in Fig. 3, using thinner Nd:YLF rod of 1 mm diameter will reduce the thermal load by almost a factor of ½ as well as stress intensity. The stress fracture limit of the YLF is in the range ~35–40 MPa [17]. Therefore, as indicated in the top left of Fig. 5 that the maximum pump power before fracture limit for the Nd:YLF of rods of diameter 4 mm, 3 mm, 2 mm and 1 mm can be pumped up 30W, 30W, 45W and 55W, respectively. These result showed that, the only way to have a significant reduced maximum stress in the Nd:YLF rod would have to use thinner crystal. Practically mounting and working with these

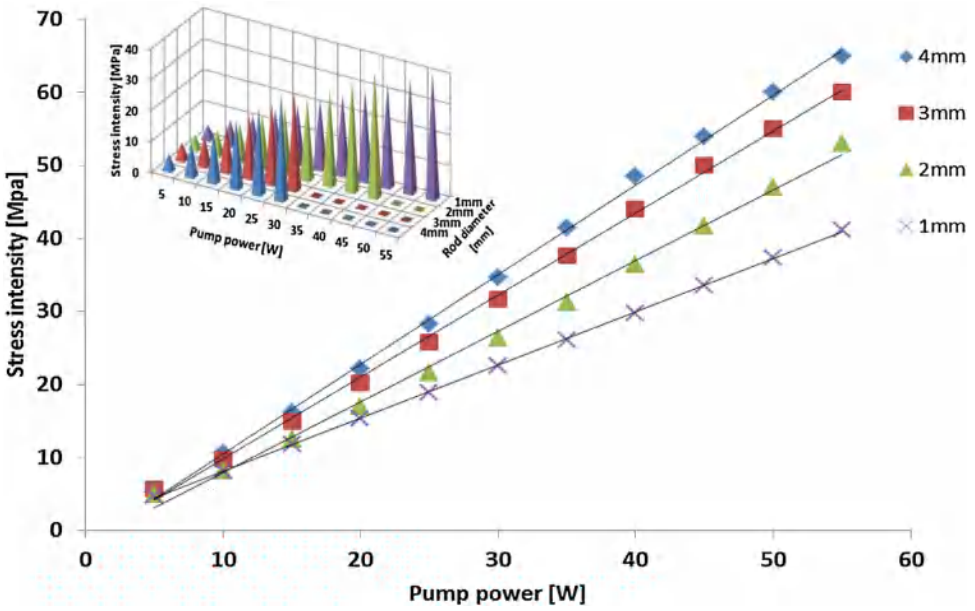

Fig. 5. Calculated maximum stress intensity versus pump power ranged from 5 to 55 W in the Nd:YLF rods of length 10 mm and different rod diameters 4 mm, 3 mm, 2 mm, and 1 mm.

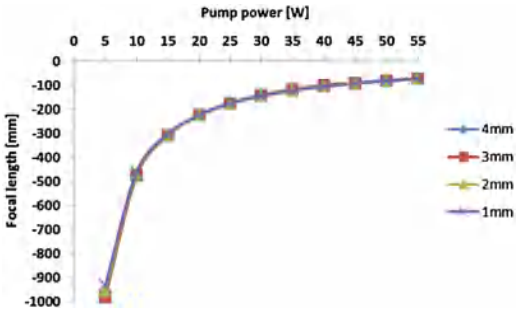

Fig. 6. Calculations of the focal length of thermally induced lens π-polarization versus pump power for rod length 10 mm and diameters 4, 3, 2 and 1 mm.

rods would have been is not difficult, we have performed laser operation in even thinner Nd:YAG crystal of radius 0.34 mm [18].

3.3. Thermally induced lens

The nonuniform temperature distribution and mechanical stress-strain results in refractive index gradients cause thermal lensing which has an adverse effect in the beam quality and divergence. As mentioned above YLF crystal is a naturally birefringent crystal, and has negative contribution to the thermally induced lens due to negative $\frac{dn_{\sigma,\pi}}{dT}$ for both polarization directions. The calculations were performed for π-polarizations because it's more pronounced than the weak thermal lens for π-polarization [2,10]. The focal length f of the thermally induced lens was calculated by fitting the optical path difference (OPD) of an ideal thin lens

$$OPD_{lens}(\mathrm{r}) = OPD_0 - \frac{1}{2 * f} \cdot r^2, \tag{2}$$

to the OPD that was calculated with the numerical simulations, where r is the distance to the rod axis and OPD_0 is the optical path difference at $r = 0$.

Fig. 6 shows the calculations of thermally induced lens in the π-polarizations rod diameters 4 mm, 3 mm, 2 mm and 1 mm verses pump powers. As can be seen in Fig. 6, the higher the pump powers the shorter focal thermal lens. During the power range of 5–55 W, the thermal focal length was in the range of 970–75 mm for all cases. It is clearly seen that, there is no change on the thermal focal lengths by reducing rod diameters. This is mainly due to quantum defect heating is the same for all cases and independent to the rod diameter.

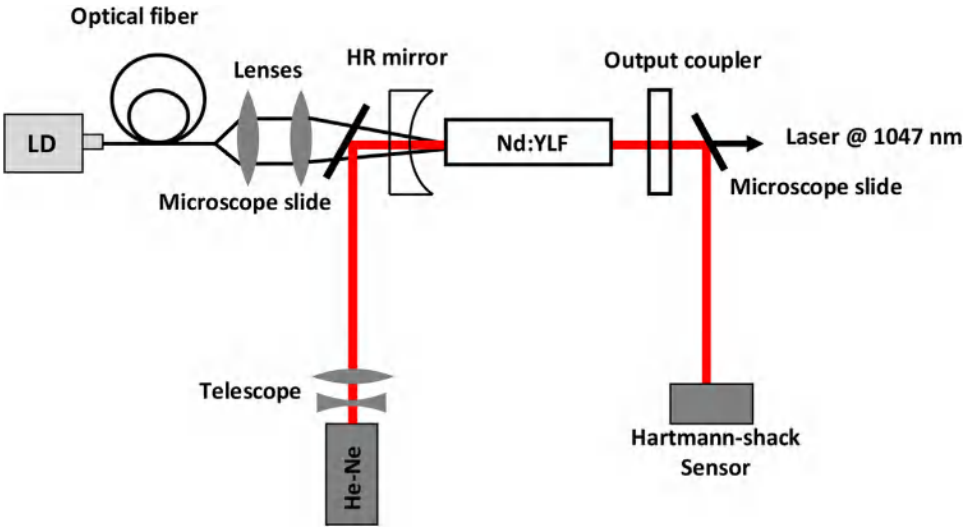

Fig. 7. Experimental setup.

4. Experimental validation of EF simulations

4.1. Experimental setup

The experimental setup is shown in Fig. 7. A fiber coupled laser diode (LD) was employed as a pump source. The focusing optics was configured to produce a circular beam spot of radius ~300 μm on the a-cut Nd:YLF laser rod as chosen in the FE simulations. An a-cut Nd:YLF crystal allows the polarization (E-field) of linearly polarized light to be either parallel or perpendicular to the c-axis. The Nd:YLF rod is 10 mm long (0.7% atom dopant) and 4 mm diameter oriented with its c-axis parallel to the resonator plane. The diode wavelength was temperature detuned from the absorption peak, at 797 nm, to longer wavelengths 805 nm to reduce the risk of rod fracture as mentioned in the simulations.

The rod is wrapped with indium foil and mounted in a copper sink. The mounted Nd:YLF rod is water cooled at 293 K and the two end faces are in contact with air. The resonator design chosen was a simple two concave-plane mirrors. The input coupling mirror is a high reflective (HR) at the wavelength near 1050 nm ($R > 99.5\%$) and high antireflective at the wavelength about 805 nm ($R < 0.5\%$). The plane output coupling mirror has 5% transmittance at ~1047 nm. The physical length of the cavity was 150 mm; a half-wave plate was added to the setup when the orthogonal polarization was required. For thermal focal length measurements, a probe He-Ne laser beam enlarged by a telescope to cover 4 mm of rod diameter and reflated to the Nd:YLF by microscope slide. The transmitted probe He-Ne laser beam reflected back to Shack-Hartmann senor (WFS1505C-Thorlabs) after passing through the Nd:YLF rod for measuring wavefront aberrations.

4.2. Experimental results

With the above setup we have obtained stable laser oscillation at maximum pump power of 30W. Under a pump power of 30 W from the laser diode, the obtained output laser at 1047 nm π-polarization was 7.2W. In order to determine the accuracy of the wavefront sensor, we performed the test measurement replacing Nd:YLF by a spherical lens of focal length f = 50 mm on translation stage. Lens focal length measurements for two different positions along probe beam axis are done, to evaluate accuracy of measurement setup. Ideally, focal length difference should be equal to distance between measurement positions. Element placement and its position determination error results in measured focal length error which varies from setup to setup, but does not exceed 11%.

Fig. 8 shows the deformation of the phase front that occurs when the He-Ne laser beam propagates through the Nd:YLF rod (a) unpumped and (b) pumped at 10W. Since most of the pump power is concentrated in the center of the rod, the lens near the centre of the rod is stronger as compared to the lens in the outer region. As can be seen in Fig. 8, that the difference between the propagation in the undisturbed and the heated rod over a range of 4 mm of the rod diameter. The dashed lines of Fig. 8 represent the fitting of the parabola presented in following equation:

$$z(x, y) = a \cdot x^2 + b \cdot y^2 + c \cdot x \cdot y + d \cdot x + e \cdot y + f \quad (2)$$

The thermal focal length is proportional to the curvature of parabola and the coefficients a and b. Depending on the pump power distribution in the laser rod, the thermal lens may not be radially symmetric. This leads to an astigmatic thermal lens with focal lengths (f_x) and (f_y). Comparison between the calculated negative focal length of thermally induced lens and the experimental measurements for Nd:YLF laser rod is presented in Table 2. The deviations between measured and calculated

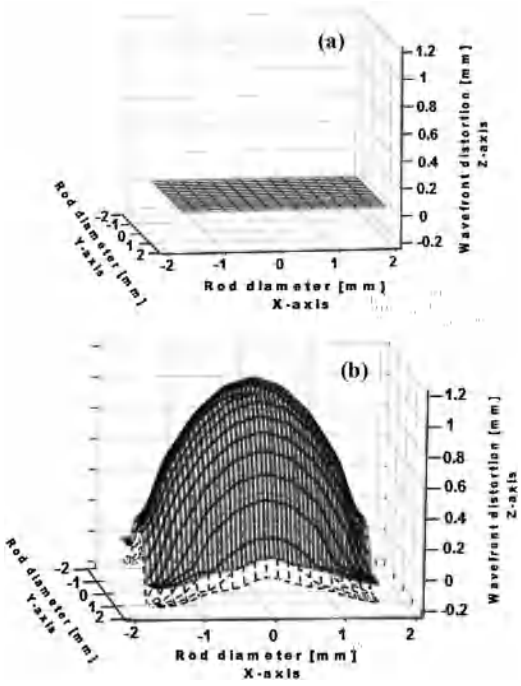

Fig. 8. Wavefront measured with Shack-Hartmann sensor after probe beam passing Nd:YLF rod (a) unpumped, (b) π-polarization pumped at 10 W.

Table 2
Comparisons between measured and calculated values of the focal length of thermally induced lens in Nd:YLF laser rod.

Pump power [W]	FE-Simulation	Shack–Hartmann	
	f_y [mm]	f_x [mm]	f_y [mm]
5	−972	−960	−950
10	−475	−465	−450
15	−308	−300	−290
20	−224	−220	−205
25	−174	−170	−160
30	−141	−135	−130

date refers to the accuracy of the FE analysis which is given by two points, on one hand by the numerical resolution of the algorithm and on the other hand by the values of the input parameters.

5. Conclusion

In conclusion, to our knowledge, this is the first report of a detailed theoretical and experimental study of power scaling of the Nd:YLF laser rod. The FE results showed that the only way to scale the power before fracture occurs in crystals of fragile nature is to use thinner crystals. In the present work we showed numerically that under the reducing Nd:YLF rod diameter by 25% would lead to scale the power limit before fracture occurs by 50% while all other parameters are fixed. Also, we have analyzed numerically temperature distributions at different pump powers and rod geometries. Central temperature and stress intensity of Nd:YLF laser rod verses pump powers is presented with clear linear dependence. The thermal focal length was calculated for laser emission at 1047 nm π-polarization and utilized to design the laser resonator. Direct measurement of dioptric powers of thermal lens using Shack-Hartmann Wavefront sensor at different pump powers is introduced. The experimental measurements were reasonably coinciding with the theoretical calculations.

Acknowledgment

The author grateful thank to the laboratories facilities of quantum optics research group (QORG) at Taif University KSA.

References

[1] W. Koechner, Solid-State Laser Engineering, Springer, 2006.
[2] A. Cousins, Temperature and thermal stress scaling in finite-length end-pumped laser rods, IEEE J. Quantum Electron. 28 (4) (1992) 1057–1069.

[3] S.C. Tidwell, J.F. Seamans, M.S. Bowers, Highly efficient 60-W TEM00 cw diode-end-pumped Nd:YAG laser, Opt. Lett. 18 (2) (1993) 116–118.
[4] J.E. Murray, Pulsed gain and thermal lensing of Nd:$LiYF_4$, IEEE J. Quantum Electron. 19 (1983) 488–491.
[5] C. Keileck, A. Hirth, M.T. Schellhorn, Ho:YAG laser intracavity pumped by a diode-pumped Tm:YLF laser, Opt. Lett. 28 (2003) 1933–1935.
[6] W. Koechner, D.K. Rice, Effect of birefringence on the performance of linearly polarized YAG: Nd lasers, IEEE J. Quantum Electron. 6 (9) (1970) 557–566.
[7] Y.J. Huang, C.Y. Tang, W.L. Lee, Y.P. Huang, S.C. Huang, Y.F. Chen, Efficient passively Q-switched Nd:YLF TEM00-mode laser at 1053 nm: selection of polarization with birefringence, Appl. Phys. B 108 (2012) 313–317.
[8] Karsten Schuhmann, Klaus Kirch, Francois Nez, Randolf Pohl, Aldo Antognini, Thin-disk laser scaling limit due to thermal lens induced misalignment instability, Appl. Opt. 55 (22) (2016) 9022–9032.
[9] Duck-Lae Kima, Byung-Tai Kimb, Laser output power losses in ceramic Nd:YAG lasers due to thermal effects, Optik 127 (2016) 9738–9742.
[10] S. Chenais, et al., Thermal lensing measurements in diode-pumped Yb doped GdCOB, YCOB YSO, YAG and KGW, Opt. Mater. 22 (2003) 129–137.
[11] S. Chenais, et al., Thermal lensing in diode-pumped ytterbium lasers part II: evaluation of quantum efficiencies and thermo-Optic coefficients, IEEE J. Quantum Electron. 40 (9) (2004) 1235–1242.
[12] P.J. Hardman, W.A. Clarkson, G.J. Friel, M. Pollnau, D.C. Hanna, Energy transfer upconversion and thermal lensing in high-power end-pumped Nd: YLF laser crystals, IEEE J. Quantum Electron. 35 (1999) 647–655.
[13] Zilong Zhang, Qiang Liu, Mingming Nie, Encai Ji, Mali Gong, Experimental and theoretical study of the weak and asymmetrical thermal lens effect of Nd:YLF crystal for σ and π polarizations, Appl. Phys. B 120 (2015) 689–696.
[14] LASCAD Gmbh, Brimhildenstr. 9, 80639 Munich, Germany, http://www.las-cad.com/index.php.
[15] Christoph Bollig, Cobus Jacobs, M.J. Daniel Esser, Edward H. Bernhardi, Hubertus M. von Bergmann, Power and energy scaling of a diode-end-pumped Nd:YLF laser through gain optimization, Opt. Express 18 (13) (2010) 13993–14003.
[16] N.U. Wetter, E.C. Sousa, F.A. Camargo, I.M. Ranieri, S.L. Baldochi, Efficient and compact diode side pumped Nd:YLF laser operating at 1053 nm with high beam quality, J. Opt. A: Pure Appl. Opt. 10 (2008) 1–5.
[17] M.E. Innocenzi, H. T.Yura, C.L. Fincher, R.A. Fields, Thermal modeling of continuous-wave end-pumped solid-state lasers, Appl. Phys. Lett. 56 (1990) 1831–1833.
[18] Sergei M. Vatnik, Reda El-Agmy, Thomas Graf, Laser operation and computation of thermal stress in end-pumped 1.1% Nd-doped yttrium aluminium garnet rods with sub-millimeter diameters, J. Mod. Opt. 18 (13) (2002) 2059–2064.